ACS APPLIED MATERIALS & INTERFACES

Research Article

Cite This: ACS Appl. Mater. Interfaces 2018, 10, 35175−35183

www.acsami.org

Assessment on the Self-Discharge Behavior of Lithium−Sulfur Batteries with $LiNO_3$-Possessing Electrolytes

Minglin Sun,[†] Xiaofei Wang,[†] Jia Wang, Hao Yang, Lina Wang,* and Tianxi Liu

State Key Laboratory for Modification of Chemical Fibers and Polymer Materials, College of Materials Science and Engineering, Innovation Center for Textile Science and Technology, Donghua University, Shanghai 201620, China

Supporting Information

ABSTRACT: It is generally understood that the reduction of nitrate on the metallic Li surface aids in the formation of a solid−electrolyte interphase. $LiNO_3$ is, therefore, frequently used as an electrolyte additive to help suppress the polysulfide redox shuttle in lithium−sulfur (Li−S) batteries. Although $LiNO_3$ enables cycling of cells with considerably improved Coulombic efficiency and cyclic performance, the self-discharge behavior has largely been neglected. We present in this work a basic but systematic study to assess self-discharge of Li−S batteries with electrolytes possessing $LiNO_3$. Comparative electrochemical tests and interfacial analysis reveal that the redox shuttle is fast enough to cause cells to self-discharge at a relatively rapid rate with limited concentration of the $LiNO_3$ additive. Despite the capacity loss of a full-charged cell under rest for one day can be controlled to 2% with $LiNO_3$ concentration as high as 0.5 M, the development of a practically viable Li−S technology looks like a daunting challenge. Further increasing $LiNO_3$ would potentially cause more irreversible reduction of $LiNO_3$ on the cathode during the first discharge. Therefore, a possible pathway for a long shelf life and low self-discharge is offered as well by the synergic protection of the separator and stabilization of the Li anode surface. The cell using a nanosized Al_2O_3-coated microporous membrane and a $LiNO_3$-possessing electrolyte exhibits an extremely suppressed self-discharge, providing an alternative perspective for the practical use of Li−S batteries.

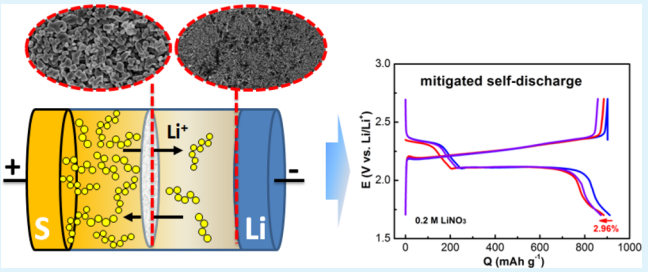

KEYWORDS: *lithium−sulfur battery, self-discharge, interface, electrolyte, separator*

1. INTRODUCTION

Thanks to the very high theoretical capacity of elemental sulfur (S_8, 1675 mA h g^{-1}) and the resource abundance, studies related to lithium−sulfur (Li−S) systems are today in the frontier of modern electrochemistry.[1] Nevertheless, the inadequate utilization of specific capacity, poor cyclic retention, severe overcharge, and self-discharge associated with the intrinsic low electrical conductivity of sulfur (5×10^{-30} S cm^{-1}) and its final reductive product of lithium sulfide (Li_2S, 10^{-13} S cm^{-1}), the safety concerns of metallic Li, and especially, the detrimental internal shuttle of soluble polysulfide species have blocked the commercialization of the Li−S technology.[2,3]

Indeed, the electrochemical lithiation of S_8 and the reverse delithiation of Li_2S are multistage processes. During the charge−discharge process, a series of lithium polysulfides with various chain lengths always form corresponding to varying reduction/oxidation stages of S_8/Li_2S. Among which, the long-chain polysulfides (Li_2S_n, $4 \leq n \leq 8$) is highly soluble in most liquid organic electrolytes with polar solvents. The migration and diffusion of Li_2S_n between the sulfur cathode and Li anode, called as the well-known "redox shuttle process", gives rise to serious loss of sulfur in the cathode, parasitic reactions on the Li anode, and degradation of both electrodes.[1−3] Preventing the shuttle and nonelectrochemical reactions of polysulfides is mainstream for tackling these obstacles. Besides the extensive efforts on exploration of functionalized sulfur cathodes,[4−10] designing of alternative electrolytes to mitigate Li_2S_n solubility is another strategy.[11−15] As a matter of fact, once the liquid organic electrolyte is used, diffusion of the continuously generated soluble polysulfide species is thermodynamically inevitable. It is a noteworthy fact that the soluble and reactive properties of Li_2S_n facilitate the smooth reaction kinetics of Li−S batteries. Suppression of their solubility comes at the cost of decreased energy efficiency and power density of batteries. To tolerate the solubility of Li_2S_n, but protect the Li anode surface should be a more feasible approach. In this case, the battery performance is greatly affected by interfacial features between the electrolyte and electrodes.

To prevent the Li metal surface from robust corrosion by Li_2S_n in the presence of electrolytes containing the $LiNO_3$ additive is the most widely adopted technique so far. Since the first introduction by Mikhaylik,[16] it has been investigated comprehensively that $LiNO_3$ is reduced to solid LiN_xO_y, Li_3N, Li_2O, and so forth, playing a pivotal role in the protective and conductive solid−electrolyte interphase (SEI)

Received: July 16, 2018
Accepted: September 25, 2018
Published: September 25, 2018

DOI: 10.1021/acsami.8b11890
ACS Appl. Mater. Interfaces 2018, 10, 35175−35183

formed on the Li anode.[17−22] As a result, the stability of the SEI layer is responsible for the defense of the polysulfide attack. Although the use of $LiNO_3$ enables cycling of cells with considerably improved Coulombic efficiency (CE) and cyclic performance, self-discharge as a critical criterion to assess batteries has largely been neglected. Self-discharge easily occurs under storage of Li−S cells with $LiNO_3$-free liquid electrolytes, especially after a full charge. The robust chemical reactions of Li_2S_n with metallic Li, stemming from the continuous migration and diffusion of Li_2S_n because of a concentration gradient, lead to the decline of the open circuit voltage (OCV) and capacity loss more or less.[23−26] Knap et al. studied the correlation of the self-discharge behavior with operational conditions, that is, the depth of discharge, idling time, and temperatures.[27] Moy et al. quantified the rate of self-discharge by measuring the shuttle currents under potentiostatic control at predetermined states of charge.[28] The Li−S cell with 1,3-dioxolane/1,2-dimethoxyethane (DOL/DME, 1/1, v/v)-based electrolytes containing 0.25 M $LiNO_3$ shows more than 1 order of magnitude of lower shuttle currents compared with that of the $LiNO_3$-free one, indicating a suppressed self-discharge. Lacey et al. explored self-discharge using similar electrolytes and confirmed $LiNO_3$ as an effective suppressant of the redox shuttle.[29] However, a capacity loss above 25% from a fully charged cell within three days suggests that the internal shuttle is far from sufficiently controlled. Wang et al. adjusted the physicochemical properties of electrolytes by adding 0.2 M $LiNO_3$ in weakly Lewis acidic/basic ionic liquid-based electrolytes.[30] Zero self-discharge was achieved for one-day storage of a fully charged cell because of polysulfide diffusion control and Li-metal passivation.

Although significant progress has been achieved, systemic studies related to self-discharge are still quite limited. This work studies whether self-discharge can be effectively mitigated or eliminated by simple adjustment of $LiNO_3$ concentration. The self-discharge rate is quantified by monitoring the OCV and capacity loss on as-assembled Li−S cells or by stopping cells mid-cycle for a period of time. In addition to scanning electron microscopy (SEM), electrochemical impedance spectroscopy (EIS) was conducted on symmetrical Li//Li cells for analysis of the Li metal/electrolyte interface. The results suggest multiple conditions should be within considerations for a practical Li−S system with low self-discharge. First, the solubility of Li_2S_n can be tolerated in the cathode environment. Second, the severe migration and diffusion of Li_2S_n across the separator should be restrained. Finally, the Li metal surface should be protected with a dense and conductive passivation layer. The synergic effect on double protection of the Li anode and separator leads to achievement of a relatively low self-discharge and high utilization of sulfur. Less than 3% capacity loss is achievable from a fully charged cell under rest for one day with an electrolyte containing 0.2 M $LiNO_3$ and a separator uniformly coated by the nanosized Al_2O_3 layer.

2. EXPERIMENTAL SECTION

2.1. Fabrication of Cathodes. In preparation of cathodes, the chemicals including sublimed sulfur (99%, Wako), Ketjenblack carbon (KB, ECP-600JD), and polyvinylidene fluoride (PVdF, HSV900) were dried thoroughly before use. A black viscous slurry consisting of 60 wt % of sulfur, 30 wt % of KB, and 10 wt % PVdF dispersed in *N*-methyl-2-pyrrolidone (NMP, ≥99.0%) was cast onto an aluminum foil (18 μm thick). Then, the electrodes were dried in vacuum at 50 °C overnight to remove NMP. Finally, the dried electrodes were punched into discs with 12 mm in diameter (d), that is, the area is 1.13 cm^2. If not specially mentioned, the average mass loading of sulfur is ∼1.20 mg, that is, the sulfur load is approximately 1.06 mg cm^{-2}. For a control experiment, electrodes with a sulfur loading of ∼3 mg cm^{-2} were also tested.

2.2. Preparation of Electrolytes. The chemicals including DOL (99.9%, J&K Scientific), DME (99.5%, Aladdin), lithium bis-(trifluoromethanesulfonyl)imide (LiTFSI, >99.95%, Aldrich), and $LiNO_3$ (99%, Alfa Aesar) were used as received. In a glove box filled with Ar (<0.1 ppm of H_2O and O_2, Mikrouna), the baseline electrolyte of DOL/DME (1/1, v/v)−1 LiTFSI was prepared as a reference. Other electrolytes with an addition of 0.01, 0.05, 0.1, 0.2, and 0.5 M $LiNO_3$ were also prepared.

2.3. Li−S and Symmetrical Li//Li Cells Assembly and Electrochemical Measurements. For assembly of Li−S cells, a sulfur cathode (d = 12 mm), two sheets of microporous membranes (Celgard, d = 16 mm, 25 μm thick), and a metallic Li anode (d = 14 mm, 0.3 mm thick) were sequentially assembled to a CR2025-type coin cell with ∼100 μL of the electrolyte. As a substitute, two sheets of commercially available Al_2O_3-coated microporous membranes (purchased from Shenzhen Kejing Star Technology, d = 16 mm, 16 μm thick) were used as well to separate the sulfur cathode and Li anode. The symmetrical Li/Li cells were assembled with a pair of metallic Li foil electrodes separated by two sheets of microporous membranes. The intention to use two sheets of membranes is to avoid any potential internal shot because of dendrite growth on the Li anode surface. Galvanostatic cycling was operated within 1.7−2.7 V (vs Li/Li^+) for Li−S cells on a Neware Battery Testing System (Shenzhen, China). For OCV comparison of as-assembled cells, voltage changes were measured as a function of storage time before any electrochemical measurement. The EIS of symmetrical Li//Li cells were measured on an electrochemical workstation (CHI 660E). The frequency range is 0.01 Hz to 1 MHz with a potentiostatic amplitude of 5 mV.

2.4. Characterizations. The microstructure and element distribution information were attained from field emission SEM (HITACHI, S-4800) combined with energy-dispersive X-ray spectroscopy (EDS). The measurement of porosity is adopted from the *n*-butanol uptake method.[31] The separator weight before and after *n*-butanol absorption for 2 h was measured. The porosity (P) is calculated on the basis of the equation: $P = [(m_b/\rho_b)/(m_b/\rho_b + m_a/\rho_a)] \times 100\%$, where m_a and m_b is the mass of the separator and *n*-butanol, and ρ_a and ρ_b are their respective densities.

3. RESULTS AND DISCUSSION

Li−S cells with simple sulfur cathodes, which are not elaborately optimized to resist self-discharge, were investigated in this work. Commercially available sulfur with a total content of 60 wt % is used as the active material in cathodes. The cathodes with a low-loading sulfur of 1 mg cm^{-2}, which may have different self-discharge behaviors with high-loading ones,[32] were investigated first in electrolytes with a $LiNO_3$ concentration of 0, 0.01, 0.05, 0.1, 0.2, and 0.5 M. To operate at a constant current density of 0.2 C (1 C = 1675 mA g^{-1}) without interruption (Figure 1), the Li−S cells with electrolytes possessing $LiNO_3$ exhibited an improved CE (defined as $Q_{charge}/Q_{discharge}$) compared to that of using the $LiNO_3$-free baseline electrolyte, being herein used as a reference. Typical stepwise voltage plateaus corresponding to the reduction from S_8 to soluble Li_2S_4 on the upper plateau (∼2.3 V vs Li/Li^+) and the subsequent transformation from Li_2S_4 to solid Li_2S on the lower plateau (∼2.1 V vs Li/Li^+) are present on the representative charge−discharge profiles (Figure S1). The baseline cell shows 130% CE in initial cycles. The severe overcharge is an apparent sign of the remarkable polysulfide shuttle. During discharge, the parasitic chemical reduction of soluble Li_2S_n on the Li metal surface would cause insufficient capacity. In recharge, the short-chain Li_2S_n generated on the

DOI: 10.1021/acsami.8b11890
ACS Appl. Mater. Interfaces 2018, 10, 35175−35183

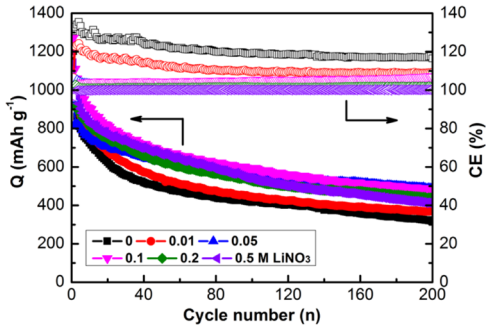

Figure 1. Cyclic performance of Li−S cells with various electrolytes presenting specific discharge capacity (Q) and CE at a current rate of 0.2 C (1 C = 1675 mA g^{-1}).

anode would shuttle back to the cathode and to be electrochemically oxidized into long-chain Li_2S_n, resulting in an overcharge. From another point of view, the robust reactions between Li_2S_n and metallic Li would also result in the deposition of insoluble Li_2S/Li_2S_2 on the anode surface, mitigating the further corrosion of Li. Thereby, approximately 118% CE is available after hundreds of cycles. However, the Li^+ ions are not allowed to move freely in the insulated Li_2S/Li_2S_2 deposition. Moreover, the surface is unstable during continuous reactions with long-chain Li_2S_n,[33] resulting in undesirable capacity fading. Addition of the 0.01 M $LiNO_3$ dose can ameliorate CE to 110% after cycles of stabilization. A CE of 105% is obtained with more $LiNO_3$ of 0.05 M, and 100% CE is reached to further increase the $LiNO_3$ concentration to 0.1, 0.2, or 0.5 M, implying the restrained polysulfide shuttle. This observation is supported further by the alleviation of capacity fading from cyclic performance.

Despite extensiveinvestigation on the shuttling-inhibiting effect by adding $LiNO_3$ in electrolytes, cyclic performance and CE do not give any specific information on the self-discharge behavior. Nevertheless, storage of a practical electronic device equipped with batteries is conventional. Self-discharge is firstly assessed by OCV evolution with rest time of as-assembled cells. The OCV of all cells show an abrupt decline within several days (Figure 2a). The OCV of the baseline cell finally holds at 2.377 V, equivalent to that with 0.01 M $LiNO_3$. A slightly increasing 0.003 V can be seen for the cell with 0.05 M $LiNO_3$ (inset of Figure 2a), and obviously higher stabilized OCV is observed by further increasing the $LiNO_3$ concentration, pointing out an alleviative self-discharge. Following storage of two weeks, variations of the first discharge profiles at 0.1 C are shown in Figure 2b. The baseline cell exhibits typical self-discharge evidenced from the considerable loss of the 2.3 V discharge plateau. A less lost upper plateau is seen by adding and increasing $LiNO_3$ concentration (inset of Figure 2b). The cell with 0.5 M $LiNO_3$ in the electrolyte displays negligible capacity lost, confirming the suppressed self-discharge. It is noteworthy that a small-sloped plateau appears obviously at 1.75 V with increased concentration of $LiNO_3$, reflecting the irreversible reduction of $LiNO_3$ on the cathode on the first discharge.[20,34] It means both Li anode and sulfur cathode consume $LiNO_3$. The reduction products of $LiNO_3$ on the Li anode promote the formation of a passivation film, whereas that on the cathode adversely affects the reversibility and capacity of the Li−S battery.[20,34] The electrochemical performance is the reflection of the two opposite and competitive roles of $LiNO_3$.

Because of a much higher reactivity of long-chain Li_2S_n, to rest the cell after a full charge always causes a rapid self-discharge.[23−30] This can be simply quantified by measuring the capacity of the cell before and after a specific rest time. Figure 3a is the discharge capacity along with corresponding CE at 0.2 C. The operation of cells was stopped upon a full charge to 2.7 V at the fifth cycle. After 24 h of storage, the cycling of cells was continued. A significant loss of discharge capacity is observed on the sixth cycle of the $LiNO_3$-free reference cell (Figure 3b), and the corresponding deteriorated CE of 140% suggests severe self-discharge during rest of the cell (Figure 3c). With respect to cells with addition of $LiNO_3$ in electrolytes, the decrease of the capacity loss with increase of $LiNO_3$ concentration can be easily distinguished. The self-discharge rate is assessed by calculating the ratio of the lost discharge capacity ($Q_{5th} - Q_{6th}$) to that on the fifth cycle (Q_{5th}), that is, $(Q_{5th} - Q_{6th})/Q_{5th}$, as can be seen from the profiles in Figure 4. In contrast to 36.35% of the baseline cell, the addition of 0.5 M $LiNO_3$ shows the most suppressed self-discharge rate of 2.07%. The recovery of the lost capacity on the second discharge after rest (Q_{7th}) calculated based on $(Q_{7th} - Q_{6th})/(Q_{5th} - Q_{6th})$, is 64, 58, 50, and 53% for the cells with a $LiNO_3$ content of 0, 0.01, 0.05, and 0.1 M, respectively. The result indicates a portion of self-discharge stemming from irreversible polysulfide shuttling, such as the reduction of Li_2S_n to insoluble Li_2S/Li_2S_2 on the Li anode, leading to the loss of active sulfur. The other part of reversible polysulfide shuttling is responsible for a significant capacity recovery. Notably, the cells with electrolytes containing 0.2 and 0.5 M $LiNO_3$ show nearly overlapped discharge profiles of the sixth and seventh cycles, indicating self-discharge is mainly ascribed to the slight loss of sulfur.

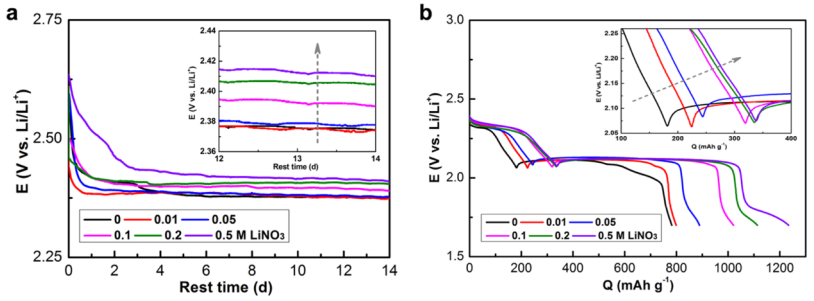

Figure 2. (a) Change in OCVs of Li−S cells with various electrolytes as a function of time. The inset is the enlargement of OCVs in the range of 12−14 days. (b) Initial discharge profiles of the cells at 0.1 C after storage for two weeks. The inset is the enlargement of voltage profiles in the range of 100−400 mA h g^{-1}.

DOI: 10.1021/acsami.8b11890
ACS Appl. Mater. Interfaces 2018, 10, 35175−35183

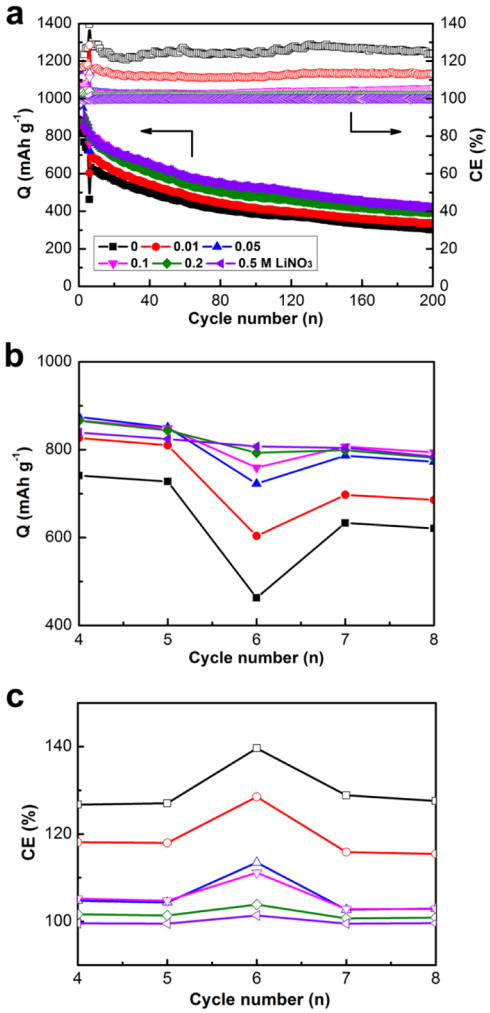

Figure 3. (a) Cyclic performance of Li−S cells presenting Q and E with various electrolytes at 0.2 C. (b,c) is the enlargement from fourth to eighth cycles in (a). After uninterrupted five cycles, the cells were rested for 24 h, and then cycled further up to 200 cycles.

It is particularly noteworthy that the formation, dissolution, migration, and diffusion of Li_2S_n intermediates that can trigger the shuttle effect are strongly time-dependent. When the movement of Li_2S_n from the cathode to anode is slower than the electrochemical reaction time, the adverse shuttle effect is reduced. Therefore, the polysulfide shuttle of a higher rate-operated Li−S cell is expected not as serious as that at a low rate. In order to observe the shuttle effect in the most extreme condition, the cell was deliberately operated at an even lower current density of 0.1 C. The baseline cell displays an equivalent self-discharge rate of 36.15% as that of 0.2 C (Figure S2a). It is surprising to see the apparently lower self-discharge rate than that at 0.2 C when $LiNO_3 \leq 0.1$ M (Figure S2b−d). Instead, a higher self-discharge rate is exhibited than that at 0.2 C with 0.2 or 0.5 M $LiNO_3$ (Figure S2e,f). For more clarification, the self-discharge rates at 0.1 and 0.2 C are summarized in Table S1. Evidently, 0.2 C is not high enough to alleviate the shuttle effect. A longer operation time, that is, a lower current rate of 0.1 C, may enable a better-formed SEI on the Li anode surface with a relatively lower concentration of $LiNO_3$. Otherwise, a higher concentration of $LiNO_3$ may enable the more effective formation of a protective layer to suppress the internal shuttle, reflected by the lower self-discharge rate at the higher rate of 0.2 C. Considering the high energy density required for practical electronic devices, electrodes with a relatively high sulfur loading of ∼3 mg cm^{-2} were also tested in the same manner. Despite suppressed self-discharge also being present with increased $LiNO_3$ in electrolytes, the general self-discharge rates are less than those of low-loading sulfur counterparts (Figure S3). For instance, the self-discharge rate is 3.23 or 0.53% for the cell with 0.2 or 0.5 M $LiNO_3$-added electrolyte, compared to 6.02 or 2.07% of low-loading sulfur electrode at 0.2 C. It can be seen that a low sulfur loading in the cells with $LiNO_3$-containing electrolytes in fact contributes further to the rate of self-discharge.

To probe electrode/electrolyte interactions and the in situ formation process of the SEI layer, EIS as a powerful technique on interfacial analysis is widely employed. However, it remains a big challenging issue to obtain a systematic interpretation on EIS spectra of Li−S cells for the extreme complexity of the system.[35−40] Taking advantage of symmetrical cells, insightful information on chemical and physical processes occurring at the electrode/electrolyte interface is available. To analyze the effect of various electrolytes on the interface between the Li electrode and electrolyte, symmetrical Li/Li cells with two identical Li electrodes are, therefore, assembled with baseline and $LiNO_3$-possessing electrolytes. From the impedance response of these Li/Li cells in Figure 5, it is seen that the spectra can be generally divided into three different frequency regions. The Ohmic resistance of the electrolyte (R_e) is responsible for the response at high frequency. The low-frequency region is ascribed to the Li^+ diffusion resistance within the electrolyte and the passivation layers building up on Li electrodes. The Li-electrode/electrolyte interfacial resistance (R_{inf}) in the Nyquist plot is indicated by the intersection of big semicircles with the real axis at middle frequency. For the high reactivity of metallic Li, the components of the electrolyte are readily decomposed on the Li-electrode surface. The SEI layer comprising the reduced products of the electrolyte is gradually formed after cell assembly. It is assumed that the thickness and also the composition of the SEI layer would change over time.[39] Consequently, R_{inf} should be varying as a function of time and electrolyte composition. As for the cell with the baseline electrolyte, R_{inf} is equal to 134 Ω right after cell assembly and continuously increasing along with time (Figure 5a). The cell with 0.01 M $LiNO_3$ follows the similar trend, except the change of R_{inf} from the 10th to 20th day becomes gradual (Figure 5b). The cell with 0.2 M $LiNO_3$ exhibits a higher initial R_{inf} of 188 Ω, and the value changes more slowly after 10 days of storage (Figure 5c). With up to 0.5 M $LiNO_3$, the initial R_{inf} is increased to 245 Ω (Figure 5d). Notably, a huge increase of the response associated with Li^+ diffusion resistance, indicated by the intersection of the semicircle with the real axis in the low-frequency region, is present. The result suggests a well-conductive passivation layer is not formed yet in the freshly assembled cell, leading to the slow diffusion of Li^+. It can be expected that a more robust reduction of a high amount of $LiNO_3$ on the Li anode surface need a longer reaction time. Surprisingly, both of the R_{inf} and Li^+ diffusion resistance greatly reduced within one day. A stable $R_{inf} \approx 130$ Ω is maintained after three days, indicating the formation of a stable SEI. The schematic cross section of the symmetrical Li/Li cells with the corresponding equivalent circuit can be modeled in Figure 5e. The R_{inf} is described by two parallel R|| constant phase element (CPE) pairs connected in series. The evolution of R_{inf} is summarized in Figure 5f, whose appearance

DOI: 10.1021/acsami.8b11890
ACS Appl. Mater. Interfaces 2018, 10, 35175−35183

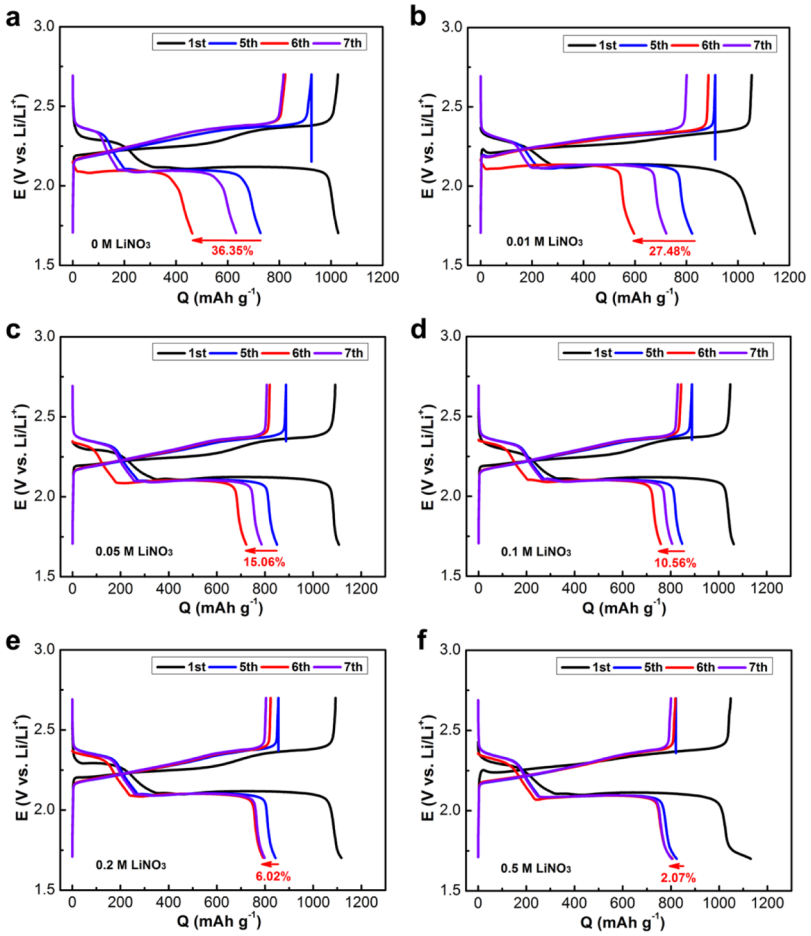

Figure 4. Representative charge−discharge voltage profiles of Li−S cells upon the first, fifth, sixth, and seventh cycles in the presence of (a) baseline and (b−f) $LiNO_3$-possessing electrolytes. After uninterrupted five cycles, the cells were rested for 24 h, and then cycled further up to 200 cycles at 0.2 C.

is dependent much on the electrolyte components. $LiNO_3$ plays a more critical role in the formation and properties of the SEI with a higher concentration.

In a Li−S cell, the interfacial properties between the Li anode and electrolyte will be altered because of the polysulfide redox shuttle effect. The morphological changes of Li metal surfaces after repeated cycles in Li−S cells are attained from SEM characterization. As is clear from Figure 6a,b, the pristine Li foil is free from any depositions on the surface layer. The cycled Li anode in the baseline cell is covered by roughly stacked deposits (Figure 6c,d). Relatively regular deposits are observed on the Li metal surface in the presence of the electrolyte with 0.1 M $LiNO_3$ (Figure 6e,f). In spite of scattered small deposits still observed, the Li metal surface of the cell with 0.5 M $LiNO_3$ reveals a much uniformed surface (Figure 6g,h), indicating the suppressed corrosion of the Li metal from the polysulfide solution. The reduced surface roughness with increased $LiNO_3$ is observed in more SEM images of the cycled Li anodes from cells with 0.01, 0.05, and 0.2 M $LiNO_3$ (Figure S4).

The above results reveal that the self-discharge of Li−S cells can be partially mitigated with a high concentration of $LiNO_3$-containing electrolytes. However, the redox shuttle is still fast enough to cause cells to self-discharge at a relatively rapid rate. Although the solubility of Li_2S_n can be tolerated in the cathode environment, the severe diffusion and migration of Li_2S_n across the separator should be restrained. For this reason, we replaced the routine microporous polymer membrane by an Al_2O_3-coated one. As depicted by SEM images, the microporous membrane exhibits uniformly interconnected elliptic pores less than 100 nm in diameter (Figure 7a,b) with a thickness of 25 μm (Figure 7c,d). Such a membrane is designed to prevent electrical shorts by keeping negative and positive electrodes apart, while allowing ionic transport between the electrodes. Apparently, the size of the pores is too large to restrain the diffusion and migration of polysulfide anions, which has a dimension <1 nm.[41] By coating the uniformly distributed nanosized Al_2O_3 on a substrate of the microporous membrane, no visible micropores can be seen (Figure 7e,f). EDS elemental mapping shows the homogeneous distribution of Al and O in the coating layer (Figure S5). The Al_2O_3 layer is ~2 μm thick on both sides of a 12 μm thick polymer membrane, leading to an overall separator thickness of 16 μm (Figure 7g,h). The well-connected interstitial voids formed between Al_2O_3 particles provide a facile pathway for ion transport. The calculated porosity of the Al_2O_3-coated microporous membrane is 64.31%, which is fairly higher than 47.46% of the routine separator. High porosity enables high electrolyte and also high soluble polysulfide uptake, which would slow down the rapid diffusion of Li_2S_n to the Li anode. The porous Al_2O_3-coating layer may serve as an efficient polysulfide diffusion barrier region to capture and retain the polysulfide species, confirmed by the much mitigated self-discharge. After uninterrupted five cycles and storage for 24 h at 0.2 C, the

DOI: 10.1021/acsami.8b11890
ACS Appl. Mater. Interfaces 2018, 10, 35175−35183

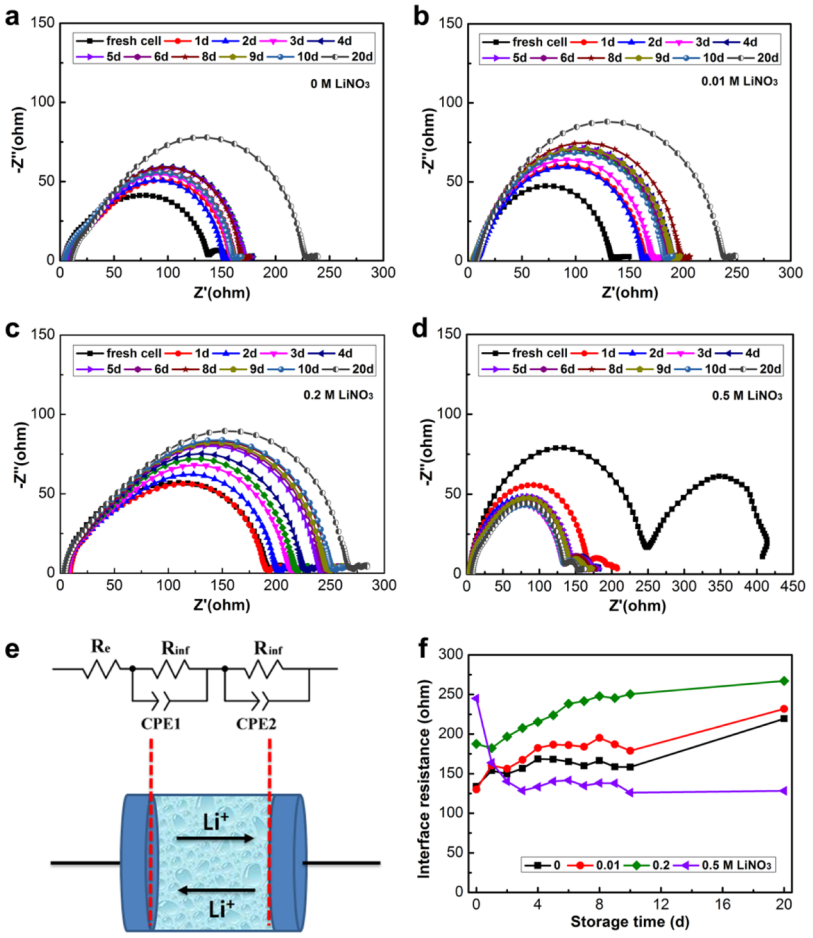

Figure 5. (a–d) Evolution of the impedance response of symmetrical Li/Li cells as a function of time in the presence of the baseline and $LiNO_3$-possessing electrolytes. (e) Schematic cross section of Li/Li cells with the corresponding equivalent circuit without taking into account the low frequency part. (f) Evolution of the values of R_{inf} as a function of time and electrolyte composition.

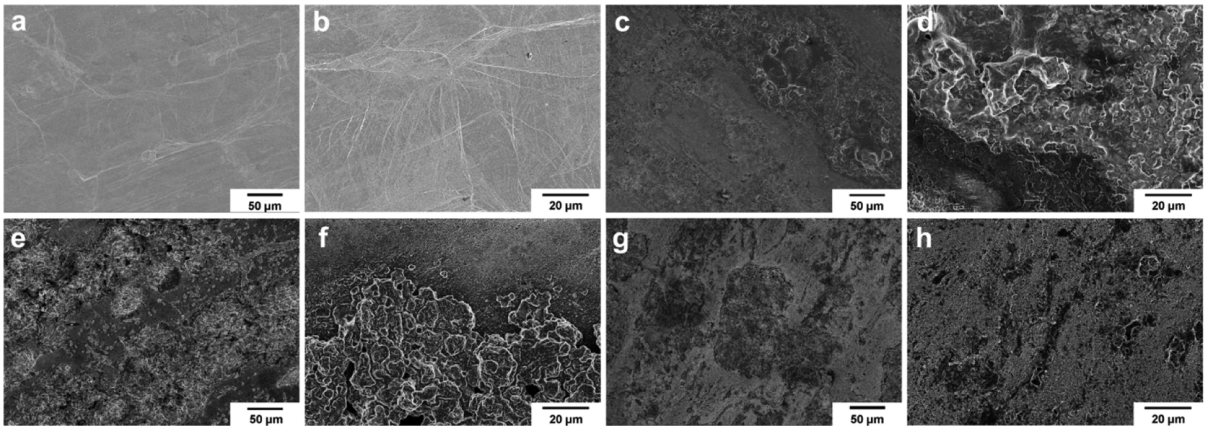

Figure 6. Surface SEM images of the (a,b) pristine Li metal and (c–h) cycled Li anodes from cells after five cycles at 0.2 C with electrolytes containing (c,d) 0 M $LiNO_3$, (e,f) 0.1 M $LiNO_3$, and (g,h) 0.5 M $LiNO_3$.

full-charged cell with the baseline electrolyte, and an addition of 0.05, 0.2, and 0.5 M $LiNO_3$ shows a self-discharge rate of 25.01, 7.69, 2.96, and 1.84%, respectively (Figure 8), in contrast to that of 36.35, 15.06, 6.02, and 2.07% with a routine separator. The effectiveness of the Al_2O_3 coating is further confirmed by the improved cyclic and rate capability using electrolytes with or without $LiNO_3$. With the baseline electrolyte, the cell employing the Al_2O_3-coated membrane holds a discharge capacity of 620 mA h g^{-1} after 100 cycles at 1 C, indicating a capacity retention of 64% (Figure S6a,b), whereas the cell with the uncoated separator delivers a capacity of 554 mA h g^{-1}, that is, a retention of 51%. With 0.2 M $LiNO_3$ in the electrolyte, a specific capacity of 668 mA h g^{-1} is remained for the cell using the Al_2O_3-coated membrane upon the 100th cycle, comparing with that of 600 mA h g^{-1} for the cell with the routine separator (Figure S6c,d). Previously,

DOI: 10.1021/acsami.8b11890
ACS Appl. Mater. Interfaces 2018, 10, 35175–35183

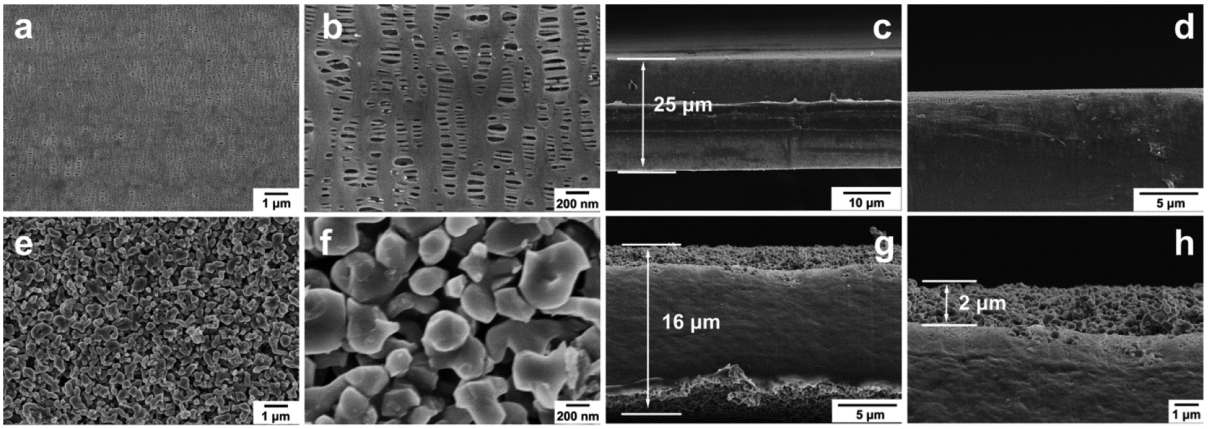

Figure 7. Surface SEM images (a,b,e,f) and cross section views (c,d,g,h) of separators. (a–d) is the routine microporous membrane, and (e–h) is the Al_2O_3-coated one with low and high magnification.

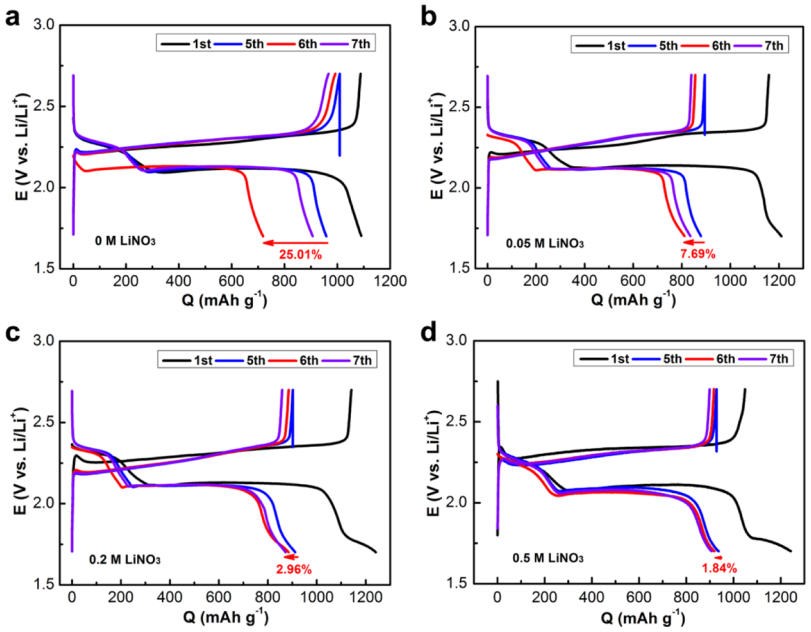

Figure 8. Representative charge–discharge voltage profiles of Li–S cells upon the first, fifth, sixth, and seventh cycles in the presence of the (a) baseline electrolyte and the electrolytes containing (b) 0.05, (c) 0.2, and (d) 0.5 M $LiNO_3$ with Al_2O_3-coated microporous membranes. After uninterrupted five cycles, the cells were rested for 24 h, and then cycled continually at 0.2 C.

promising Li–S batteries have been reported with a graphene and Al_2O_3 doubly coated polypropylene separator[42] or a Al_2O_3 one-side-coated porous separator,[43] however, self-discharge performance has been neglected. The results presented herein suggest the double protection of the separator and Li metal surface is beneficial for improved Li–S batteries with low self-discharge and long shelf life.

4. CONCLUSIONS

A better understanding of Li–S chemistry related to the self-discharge behavior is constituted by our work. It is not viable for a practical Li–S battery to only depend on the passivation of the Li anode surface with electrolytes containing the $LiNO_3$ additive. For one-day storage following a full charge, the self-discharge rate can be controlled to 2.07% with a low-loading and 0.53% with a high-loading sulfur electrode for the cells with a 0.5 M $LiNO_3$-added electrolyte. Obviously, a longer term storage would induce a more severe self-discharge. A more high content of $LiNO_3$ would bring new concerns, like the adverse reduction of $LiNO_3$ on the cathode, the high viscosity of electrolytes, the robust consumption of Li, and so forth. The demonstration of double protection of the Li anode and separator provides a promising candidate approach for developing practical Li–S batteries with a long shelf life and low self-discharge.

■ ASSOCIATED CONTENT

Supporting Information

The Supporting Information is available free of charge on the ACS Publications website at DOI: 10.1021/acsami.8b11890.

Representative charge–discharge profiles of Li–S cells, summary of self-discharge rates in the presence of various electrolytes at rates of 0.1 and 0.1 C, self-discharge behavior with high-loading sulfur electrodes, more SEM images of the cycled Li anode surface, EDS elemental mapping of the Al_2O_3-coated microporous membrane, and cyclic performance of cells with different separators at a high rate of 1 C (PDF)

DOI: 10.1021/acsami.8b11890
ACS Appl. Mater. Interfaces 2018, 10, 35175–35183

AUTHOR INFORMATION

Corresponding Author

*E-mail: linawang@dhu.edu.cn.

ORCID

Lina Wang: 0000-0002-2211-4661

Author Contributions

†M.S. and X.W. contributed equally.

Notes

The authors declare no competing financial interest.

ACKNOWLEDGMENTS

The authors acknowledge funding support from the National Natural Science Foundation of China (21603030), the Natural Science Foundation of Shanghai (17ZR1446400), and the Fundamental Research Funds for the Central Universities (2232018D3-02).

REFERENCES

(1) Bruce, P. G.; Freunberger, S. A.; Hardwick, L. J.; Tarascon, J. M. Li−O_2 and Li−S Batteries with High Energy Storage. *Nat. Mater.* **2011**, *11*, 19−29.

(2) Choi, N.-S.; Chen, Z.; Freunberger, S. A.; Ji, X.; Sun, Y.-K.; Amine, K.; Yushin, G.; Nazar, L. F.; Cho, J.; Bruce, P. G. Challenges Facing Lithium Batteries and Electrical Double-Layer Capacitors. *Angew. Chem., Int. Ed. Engl.* **2012**, *51*, 9994−10024.

(3) Manthiram, A.; Fu, Y.; Su, Y.-S. Challenges and Prospects of Lithium−Sulfur Batteries. *Acc. Chem. Res.* **2013**, *46*, 1125−1134.

(4) Wu, X.-W.; Xie, H.; Deng, Q.; Wang, H.-X.; Sheng, H.; Yin, Y.-X.; Zhou, W.-X.; Li, R.-L.; Guo, Y.-G. Three-Dimensional Carbon Nanotubes Forest/Carbon Cloth as an Efficient Electrode for Lithium−Polysulfide Batteries. *ACS Appl. Mater. Interfaces* **2017**, *9*, 1553−1561.

(5) Zhang, J.; Yang, C.-P.; Yin, Y.-X.; Wan, L.-J.; Guo, Y.-G. Sulfur Encapsulated in Graphitic Carbon Nanocages for High-Rate and Long-Cycle Lithium−Sulfur Batteries. *Adv. Mater.* **2016**, *28*, 9539−9544.

(6) Lee, J. S.; Manthiram, A. Hydroxylated N-doped Carbon Nanotube-Sulfur Composites as Cathodes for High-Performance Lithium−Sulfur Batteries. *J. Power Sources* **2017**, *343*, 54−59.

(7) Pang, Q.; Liang, X.; Kwok, C. Y.; Nazar, L. F. Review-The Importance of Chemical Interactions between Sulfur Host Materials and Lithium Polysulfides for Advanced Lithium−Sulfur Batteries. *J. Electrochem. Soc.* **2015**, *162*, A2567−A2576.

(8) Li, Y.; Ye, D.; Liu, W.; Shi, B.; Guo, R.; Zhao, H.; Pei, H.; Xu, J.; Xie, J. A MnO_2/Graphene Oxide/Multi-Walled Carbon Nanotubes-Sulfur Composite with Dual-Efficient Polysulfide Adsorption for Improving Lithium−Sulfur Batteries. *ACS Appl. Mater. Interfaces* **2016**, *8*, 28566−28573.

(9) Chen, M.; Jiang, S.; Cai, S.; Wang, X.; Xiang, K.; Ma, Z.; Song, P.; Fisher, A. C. Hierarchical Porous Carbon Modified with Ionic Surfactants as Efficient Sulfur Hosts for the High-Performance Lithium−Sulfur Batteries. *Chem. Eng. J.* **2017**, *313*, 404−414.

(10) Wang, L.; Zhao, Y.; Thomas, M. L.; Byon, H. R. In Situ Synthesis of Bipyramidal Sulfur with 3D Carbon Nanotube Framework for Lithium−Sulfur Batteries. *Adv. Funct. Mater.* **2014**, *24*, 2248−2252.

(11) Suo, L.; Hu, Y.-S.; Li, H.; Armand, M.; Chen, L. A New Class of Solvent-in-Salt Electrolyte for High-Energy Rechargeable Metallic Lithium Batteries. *Nat. Commun.* **2013**, *4*, 1481.

(12) Wang, L.; Byon, H. R. N-Methyl-N-propylpiperidinium bis(trifluoromethanesulfonyl)imide-Based Organic Electrolyte for High Performance Lithium-−Sulfur Batteries. *J. Power Sources* **2013**, *236*, 207−214.

(13) Yang, W.; Yang, W.; Song, A.; Gao, L.; Sun, G.; Shao, G. Pyrrole as a Promising Electrolyte Additive to Trap Polysulfides for Lithium−Sulfur Batteries. *J. Power Sources* **2017**, *348*, 175−182.

(14) Chen, S.; Dai, F.; Gordin, M. L.; Yu, Z.; Gao, Y.; Song, J.; Wang, D. Functional Organosulfide Electrolyte Promotes an Alternate Reaction Pathway to Achieve High Performance in Lithium−Sulfur Batteries. *Angew. Chem., Int. Ed. Engl.* **2016**, *55*, 4231−4235.

(15) Wu, H.-L.; Shin, M.; Liu, Y.-M.; See, K. A.; Gewirth, A. A. Thiol-Based Electrolyte Additives for High-Performance Lithium−Bulfur batteries. *J. Power Sources* **2017**, *32*, 50−58.

(16) Mikhaylik, Y. V. Electrolytes for Lithium Sulfur Cells. U.S. Patent 7,354,680 B2, 2008.

(17) Aurbach, D.; Pollak, E.; Elazari, R.; Salitra, G.; Kelley, C. S.; Affinito, J. On the Surface Chemical Aspects of Very High Energy Density, Rechargeable Li−Sulfur Batteries. *J. Electrochem. Soc.* **2009**, *156*, A694−A702.

(18) Xiong, S.; Xie, K.; Diao, Y.; Hong, X. Properties of Surface Film on Lithium Anode with $LiNO_3$ as Lithium Salt in Electrolyte Solution for Lithium−Sulfur Batteries. *Electrochim. Acta* **2012**, *83*, 78−86.

(19) Liang, X.; Wen, Z.; Liu, Y.; Wu, M.; Jin, J.; Zhang, H.; Wu, X. Improved Cycling Performances of Lithium Sulfur Batteries with $LiNO_3$-Modified Electrolyte. *J. Power Sources* **2011**, *196*, 9839−9843.

(20) Zhang, S. S. Role of $LiNO_3$ in Rechargeable Lithium/Sulfur Battery. *Electrochim. Acta* **2012**, *70*, 344−348.

(21) Ding, N.; Zhou, L.; Zhou, C.; Geng, D.; Yang, J.; Chien, S. W.; Liu, Z.; Ng, M.-F.; Yu, A.; Hor, T. S. A.; Sullivan, M. B.; Zong, Y. Building Better Lithium−Sulfur Batteries: from $LiNO_3$ to Solid Oxide Catalyst. *Sci. Rep.* **2016**, *6*, 33154.

(22) Zhang, S. S. A New Finding on the Role of $LiNO_3$ in Lithium−Sulfur Battery. *J. Power Sources* **2016**, *322*, 99−105.

(23) Rauh, R. D.; Abraham, K. M.; Pearson, G. F.; Surprenant, J. K.; Brummer, S. B. A Lithium/Dissolved Sulfur Battery with an Organic Electrolyte. *J. Electrochem. Soc.* **1979**, *126*, 523−527.

(24) Cheon, S.-E.; Ko, K.-S.; Cho, J.-H.; Kim, S.-W.; Chin, E.-Y.; Kim, H.-T. Rechargeable Lithium Sulfur Battery. *J. Electrochem. Soc.* **2003**, *150*, A796−A799.

(25) Mikhaylik, Y. V.; Akridge, J. R. Polysulfide Shuttle Study in the Li/S Battery System. *J. Electrochem. Soc.* **2004**, *151*, A1969−A1976.

(26) Chung, S.-H.; Han, P.; Manthiram, A. Quantitative Analysis of Electrochemical and Electrode Stability with Low Self-Discharge Lithium−Sulfur Batteries. *ACS Appl. Mater. Interfaces* **2017**, *9*, 20318−20323.

(27) Knap, V.; Stroe, D.-I.; Swierczynski, M.; Teodorescu, R.; Schaltz, E. Investigation of the Self-Discharge Behavior of Lithium−Sulfur Batteries. *J. Electrochem. Soc.* **2016**, *163*, A911−A916.

(28) Moy, D.; Manivannan, A.; Narayanan, S. R. Direct Measurement of Polysulfide Shuttle Current: A Window into Understanding the Performance of Lithium−Sulfur Cells. *J. Electrochem. Soc.* **2014**, *162*, A1−A7.

(29) Lacey, M. J.; Yalamanchili, A.; Maibach, J.; Tengstedt, C.; Edström, K.; Brandell, D. The Li−S battery: an Investigation of Redox Shuttle and Self-Discharge Behaviour with $LiNO_3$-Containing Electrolytes. *RSC Adv.* **2016**, *6*, 3632−3641.

(30) Wang, L.; Liu, J.; Yuan, S.; Wang, Y.; Xia, Y. To Mitigate Self-Discharge of Lithium−Sulfur Batteries by Optimizing Ionic Liquid Electrolytes. *Energy Environ. Sci.* **2016**, *9*, 224−231.

(31) Zhang, J.; Yue, L.; Kong, Q.; Liu, Z.; Zhou, X.; Zhang, C.; Xu, Q.; Zhang, B.; Ding, G.; Qin, B.; Duan, Y.; Wang, Q.; Yao, J.; Cui, G.; Chen, L. Sustainable, Heat-Resistant and Flame-Retardant Cellulose-Based Composite Separator for High-Performance Lithium Ion Battery. *Sci. Rep.* **2014**, *4*, 3935.

(32) Gordin, M. L.; Dai, F.; Chen, S.; Xu, T.; Song, J.; Tang, D.; Azimi, N.; Zhang, Z.; Wang, D. Bis(2,2,2-trifluoroethyl) Ether As an Electrolyte Co-solvent for Mitigating Self-Discharge in Lithium−Sulfur Batteries. *ACS Appl. Mater. Interfaces* **2014**, *6*, 8006−8010.

(33) Wang, L.; Wang, Y.; Xia, Y. A High Performance Lithium-Ion Sulfur Battery Based on a Li_2S Cathode Using a Dual-Phase Electrolyte. *Energy Environ. Sci.* **2015**, *8*, 1551−1558.

(34) Zhang, S. S. Effect of Discharge Cutoff Voltage on Reversibility of Lithium/Sulfur Batteries with $LiNO_3$-Contained Electrolyte. *J. Electrochem. Soc.* **2012**, *159*, A920−A923.

DOI: 10.1021/acsami.8b11890
ACS Appl. Mater. Interfaces 2018, 10, 35175−35183

(35) Cañas, N. A.; Hirose, K.; Pascucci, B.; Wagner, N.; Friedrich, K. A.; Hiesgen, R. Investigations of Lithium−Sulfur Batteries Using Electrochemical Impedance Spectroscopy. *Electrochim. Acta* **2013**, *97*, 42−51.
(36) Deng, Z.; Zhang, Z.; Lai, Y.; Liu, J.; Li, J.; Liu, Y. Electrochemical Impedance Spectroscopy Study of a Lithium/Sulfur Battery: Modeling and Analysis of Capacity Fading. *J. Electrochem. Soc.* **2013**, *160*, A553−A558.
(37) Yuan, L.; Qiu, X.; Chen, L.; Zhu, W. New Insight into the Discharge Process of Sulfur Cathode by Electrochemical Impedance Spectroscopy. *J. Power Sources* **2009**, *189*, 127−132.
(38) Kolosnitsyn, V. S.; Kuzmina, E. V.; Karaseva, E. V.; Mochalov, S. E. A Study of the Electrochemical Processes in Lithium−Sulphur Cells by Impedance Spectroscopy. *J. Power Sources* **2011**, *196*, 1478−1482.
(39) Conder, J.; Villevieille, C.; Trabesinger, S.; Novák, P.; Gubler, L.; Bouchet, R. Electrochemical Impedance Spectroscopy of a Li−S battery: Part 1. Influence of the Electrode and Electrolyte Compositions on the Impedance of Symmetric Cells. *Electrochim. Acta* **2017**, *244*, 61−68.
(40) Conder, J.; Villevieille, C.; Trabesinger, S.; Novák, P.; Gubler, L.; Bouchet, R. Electrochemical Impedance Spectroscopy of a Li−S battery: Part 2. Influence of Separator Chemistry on the Lithium Electrode/Electrolyte Interface. *Electrochim. Acta* **2017**, *255*, 379−390.
(41) Xin, S.; Gu, L.; Zhao, N.-H.; Yin, Y.-X.; Zhou, L.-J.; Guo, Y.-G.; Wan, L.-J. Smaller Sulfur Molecules Promise Better Lithium−Sulfur Batteries. *J. Am. Chem. Soc.* **2012**, *134*, 18510−18513.
(42) Hwang, J.-Y.; Kim, H. M.; Shin, S.; Sun, Y.-K. Designing a High-Performance Lithium-Sulfur Batteries Based on Layered Double Hydroxides-Carbon Nanotubes Composite Cathode and a Dual-Functional Graphene-Polypropylene-Al_2O_3 Separator. *Adv. Funct. Mater.* **2018**, *28*, 1704294.
(43) Zhang, Z.; Lai, Y.; Zhang, Z.; Zhang, K.; Li, J. Al_2O_3-Coated Porous Separator for Enhanced Electrochemical Performance of Lithium Sulfur Batteries. *Electrochim. Acta* **2014**, *129*, 55−61.

DOI: 10.1021/acsami.8b11890
ACS Appl. Mater. Interfaces 2018, 10, 35175−35183